

An Internet of Things-based Self-Correcting Fused Deposition Modeling Monitoring System

Dhruv Shah¹, Sarah Malik¹, Hadi Khezam¹, Pablo Huang¹, Rakeen Rouf¹, Yolanda Mack², and Antonios Kotsos^{1*}

ABSTRACT

Additive manufacturing (AM) processes such as fused deposition modeling (FDM) provide versatile manufacturing capabilities, but due to variability of environmental conditions as well as inherent process variations, parts produced on desktop-class FDM printers are often riddled with defects. In the FDM process, layers of polymer material are deposited in specific patterns to produce parts with complex geometries without the need for extensive post processing. During this deposition process, however, there are several factors including temperature and vibrations that can cause defects. The present project develops a workflow to monitor and control AM processes that utilize a closed-loop, in-situ sensory feedback system that actively adjusts operational parameters based on sensor inputs in the framework of recent digital twin examples. The project was developed using a commercially available FDM 3D-printer outfitted with acoustic emission (AE) sensors to develop an IoT-based testbed for manufacturing process monitoring and control. Three principal components were incorporated in this system: the manufacturing process, a sensing approach, and an IoT interface. For this project, AE data was collected during a live FDM process. Several test prints were conducted to establish a threshold of acquired signals that could be used to classify the state of the part as one without notable flaws (“pristine”) and one with flaws (“defective”). Common FDM defects, such as under- and over-extrusion where there is too little or too much material flow, were purposefully seeded in the G-Code that was used to run the print. The obtained thresholds were used to define an alarm trigger that would intercept the running G-Code with a correction script to prevent the severity of the defect from increasing. The overall control loop was able to detect the defective state of the printer using the acquired AE signals, use the pre-defined alarm thresholds to trigger a correction script, and control the printer by means of the IoT interface. The described workflow is modularized to accommodate different processes and additional sensing methods.

Keywords

Internet of Things (IoT), 3D Print Monitoring, Acoustic Emission, Intelligent System, Damage Assessment, Self-Correcting Manufacturing.

¹ Mechanical Engineering & Mechanics, Theoretical & Applied Mechanics Group/Drexel University, Philadelphia, PA, 19104, USA

² Raytheon Technologies Corporation, Attn: M09 ReyWest Receiving, 3350 Hemisphere Loop, M09 Dock, Tucson AZ 85706.

* Corresponding Author: Prof. Antonios Kotsos, Tel: +1 215 895 2297, E-mail: ak866@drexel.edu

Introduction

The fourth industrial revolution (Industry 4.0) is characterized by a manufacturing paradigm focused on the interconnectivity, automation, smart-monitoring, and real-time insights of industrial systems. With the advent of Industry 4.0, modern manufacturing and production processes capitalize on real-time diagnostics using edge-computing coupled with signal processing and machine learning (ML) algorithms to dynamically assess and improve system performance (Commission, 2021; Kennedy, 2015). When coupled with cloud computing and artificial intelligence (AI) methods, such diagnostics can help efficiently reroute processes and redeploy personnel to minimize impact on production lines due to failures, issues, or equipment maintenance, thus achieving the goal of data-driven prognostics. In this context, the present work developed a workflow to monitor and control advanced manufacturing (AM) processes by utilizing a closed-loop, in-situ sensory feedback system that actively adjusts operational parameters based on sensor inputs.

To achieve such coupling between diagnostics and prognostics in realistic conditions where the production time is of importance, there is a need for real-time data processing for automated systems. Current data handling and processing mechanisms are designed based on traditionally collected information and may consist of several non-integrated systems, even in the context of built-in controls. To address this issue, an Internet of Things (IoT) workflow provides the connection between cloud services and real-time data integration, enhanced by machine learning algorithms.

An AM process such as fused deposition modeling (FDM) is a mainstream manufacturing process used for prototyping of complex components (H. Wu, Wang, & Yu, 2016). Despite their capabilities, FDM-type 3D-printers require a relatively long time to manufacture parts, utilizing a heated deposition unit to add sequential layers of polymer in layered profiles to achieve complex

geometries. Given the time involvement for part production, 3D-printing technologies would benefit from automated feedback and assessment of the part as it is being manufactured to address manufacturing defects. Several of these defects are associated with the temperature and motion settings of the printer during the manufacturing process. These defects include warping of parts, under/over extrusion of material throughout layers, and misalignment due to external vibrations or slippage of the printer's movement axes (**Figure 1**), to name a few. The severity of a defect can be reduced by correcting/intercepting the manufacturing process at the onset of the defect. This offers economically conscious options for large scale manufacturing operations by augmenting the existing manufacturing process with sensory feedback and control.

Example of 3D-Printing Defects



Figure 1: Common defects in FDM-type 3D-printing. From left to right: stringing (Excess material deposition during travel to next location), under-extrusion (Less material deposition than required), over-extrusion (More material deposition than required)

To detect the presence of a defect, a sensing methodology is needed to capture relevant information as it pertains to the machine and the part that is being produced. Efforts have been reported, specifically in the context of FDM-type printing, to acquire relevant data using thermal, vibrational, and acoustic sensors (Fu, Downey, Yuan, Pratt, & Balogun, 2020). Such sensing devices are typically extrinsic to the on-board capabilities of traditional 3D-printers. Some

researchers are using built-in sensing technology to detect faults, while others are leveraging non-destructive evaluation (NDE) techniques adapted for AM purposes (Bacha, Sabry, & Benhra, 2019; Lu & Wong, 2018; Yoon, He, & Van Hecke, 2014). For example, approaches involving infrared thermography attempt to extract part layer temperature and distinguish between normal and abnormal states (Ferraris, Zhang, & Van Hooreweder, 2019). Material extrusion states such as loading, normal, and jammed were differentiated based on measured current-draw of the feeder mechanism/extruder (Tlegenov, Lu, & Hong, 2019). In addition, Rao et al. measured vibration on the build platform of an FDM printer using accelerometers to gauge proper extrusion and adhesion (Rao, Liu, Roberson, Kong, & Williams, 2015).

Another relevant sensing method that has proven useful in multiple monitoring applications is acoustic emission (AE), a method typically used for NDE. In the context of polymer 3D-printers, AE sensors have been used to acquire raw acoustic data in the form of voltage signals and process them on a data acquisition unit to obtain extracted features that can be further analyzed for postmortem assessment of the print. Other researchers used AE in a qualitative capacity to assess the health of the machine as opposed to the health of the part (Liu, Hu, Wu, & Wang, 2018; H. Wu, Y. Wang, et al., 2016). For example, efforts by Wu et al. involved a data-driven monitoring and diagnostic method that used AE sensors to detect failure modes of a 3D-printer's first layer, which is often considered the most important layer to ensure proper adhesion to the build platform and thereby yielding a successful print (H. Wu, Yu, & Wang, 2019). Overall, the major drive for monitoring FDM printer processes as seen in literature has been to reach the level of a model-based approach, which accounts for all relevant process parameters, and interprets them in a manner capable of informing structural data in post-manufacturing mechanical tests (Fu et al.,

2020). This is currently a resource-intensive approach which requires hybridized methods with multiple sensors providing data to reliably predict and classify both printer and part health.

IoT has been used for 3D-print monitoring to address various challenges with manufacturing operations management. For example, the integration of IoT in 3D-printing for logistical optimization was recently proposed (Chen & Wang, 2019) to minimize the cycle time for manufacturing by effectively optimizing the overall workload of receiving customer orders, finding manufacturing availability in certain facilities, and delivering the order to the customer in a timely fashion. The integration of a cloud-based platform to enhance product lifecycle management that connects not only 3D-printers and materials, but also test data and knowledgebase was also reported (Y. Wang, Lin, Zhong, & Xu, 2019). Cloud data for AM has also been used to connect the product model with a bill of processes, customer orders, and manufacturing operations (Do, 2017).

For 3D-print monitoring, sensing technologies to improve prints have also been a critical research area. Defect detection approaches for 3D-print monitoring have used both AE and visual techniques (Delli & Chang, 2018; Gaja & Liou, 2017; M. Wu, Phoha, Moon, & Belman, 2016). Machine learning approaches to damage detection have also been implemented offline to characterize faults during the print process (Bacha et al., 2019; Meng et al., 2020; Menon, Póczos, Feinberg, & Washburn, 2019; C. Wang, Tan, Tor, & Lim, 2020).

The important need for a closed-loop feedback 3D-print monitoring system has been introduced by a number of publications using NDE sensing (Garanger, Khamvilai, & Feron, 2018; H. Wu, Y. Wang, et al., 2016; H. Wu, Yu, & Wang, 2016). Specifically, Reese et al. published a patent for real-time monitoring and additional tool path correction instructions during the 3D-printing process (Reese, Bheda, & Mondesir, 2019). The system output is a corrected physical

print accompanied by a report containing 3D space displays, structural geometry, and inherent properties of the final object. An implementation of combining image processing, neural networks, and closed loop control has also been implemented for an ink-jet based 3D-printer where the voltage is adjusted based on the current droplet analysis (T. Wang, Kwok, Zhou, & Vader, 2018). Another closed loop system for additive manufacturing was implemented by Breese et al. in which the powder mass flow rate is adjusted based on an optical powder flow sensor in the context of laser metal deposition (Breese, Hauser, Regulin, Seebauer, & Rupprecht, 2021). A series of other closed loop systems in academia and commercial products for additive manufacturing have been reviewed by Rivera et. al in which the goal is to reduce the possibility of mistakes and overall reliability of the system (Rivera & Arciniegas, 2020).

The overall objective of the present work is to develop an IoT framework to detect and correct manufacturing defects. More specifically, a commercially available 3D-printer outfitted with passive acoustic sensors was used to develop an IoT-based testbed for manufacturing process monitoring and control.

Approach & Methods

The proposed testbed has three principal components: a manufacturing process, a sensing approach, and IoT functionality. The IoT interface serves to interconnect the manufacturing process and the sensing data, resulting in a real-time closed loop monitoring and control system. An FDM 3D-printer is used as the manufacturing methodology for the monitoring system and AE sensors were utilized to acquire acoustic data for sensing analysis. **Figure 2** is the global overview of the IoT-based interconnectivity between the 3D-printing manufacturing system and AE-derived sensing.

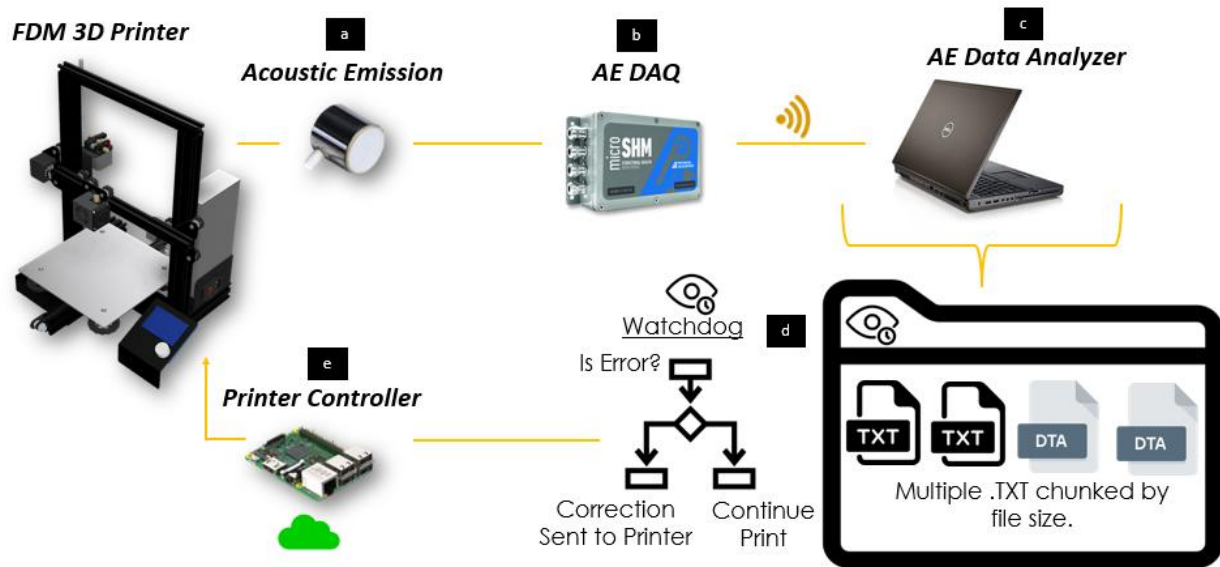


Figure 2: IoT approach to achieve closed-loop control with (a) acoustic emission sensor mounted on the 3D-printer, (b) corresponding AE DAQ, and (c) AE Data Analyzer to view and read the sensing files with (d) a watchdog script. The printer controller (e) sends the correction command to the 3D-printer.

Additive Manufacturing System

For the purposes of this work, the Ender™ 3 Pro (Creality3D, Shenzhen, China) 3D-printer was selected for its configurability and addition of components due to its open framework design (**Figure 3**). The Ender™ 3 Pro has a 220x220x250mm build volume, 0.1mm XY-axis accuracy, 0.1-0.4 mm layer resolution, 0.4mm nozzle diameter, and a maximum printing speed of 180mm/s. The 3D-printer uses a single print head and consumes 1.75mm diameter thermoplastic filaments such as polylactic acid (PLA), thermoplastic polyurethane (TPU), and acrylonitrile butadiene styrene (ABS). This study utilized primarily PLA, commonly used for consumer 3D-printing due to its low relative cost and high print success rate.

Creality Ender 3 Pro	
Printer Type	Fused Deposition Modeling (FDM)
Build Volume	220 x 220 x 250 mm
Print Head	Single
XY Axis Accuracy	0.1 mm
Print Speed	180 mm/s
Nozzle Diameter	0.4 mm
Consumables	1.75 mm PLA, TPU, ABS
Layer Resolution	0.1 - 0.4 mm

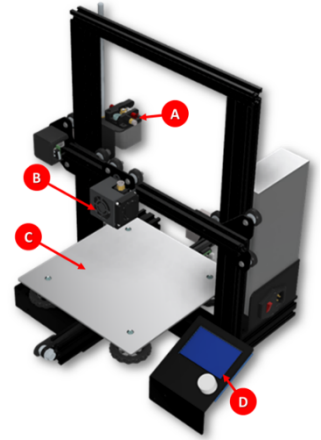


Figure 3: Specifications of Ender™ 3 Pro FDM-type 3D-Printer, which is equipped with a (a) material feeder/extruder, (b) high-temp nozzle deposition unit, (c) heated build platform, and (d) on-board controller interface.

Testing Geometry

To identify signal differences between a 3D-print with no notable flaws, referred to as “pristine”, and a print characterized by evident issues, denoted as “defective”, signal analysis was performed on a predefined dataset described in Experimental Approach to determine the value of an alarm threshold. The 3D-printed testing geometry used to experimentally determine the alarm threshold was the hollow trapezoidal geometry (**Figure 4**). The hollow feature of the geometry was incorporated to reduce print time and eliminate effects from internal defects due to the infill pattern. The trapezoidal test geometry was created using a computer-aided design software, (Fusion 360, Autodesk™, San Rafael, CA), converted into a tessellated triangular mesh (*.stl file format), and further transcribed into machine code (G-Code) using slicer software (3D-printer dependent). The G-Code produced by the slicer software contains commands related to motion, speed, extrusion rate, and temperature, among other instructions.

To obtain acoustic signals pertaining to defective prints, “over-“ and “under-“ extrusion defects were purposefully instigated in specific layers of the trapezoidal test geometry via a modified G-Code file. More specifically, the extruder flow rate was purposefully adjusted to 150% and 35% to simulate over- and under-extrusion, respectively. The percentage changes in flowrate

were chosen purposefully as to not clog the nozzle while printing. The pristine trapezoidal part was printed at a default 100% flow rate setting. The geometry was manufactured with PLA filament at nozzle and bed temperatures of 205 °C and 61 °C, respectively. The layer height was set to 0.2mm resolution with three perimeters/shells and a relatively slow print speed of 20 mm/s.

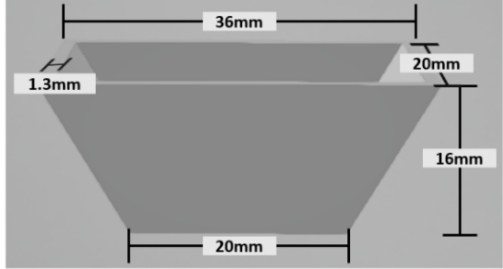
Trapezoidal Structure		
Material	Polylactic Acid (PLA)	
Hot End Temperature	205 °C	
Bed Temperature	61 °C	
Layer Height	0.2 mm	
Print Speed	20 mm/s	
# Perimeters	3	

Figure 4: Print parameters of the trapezoidal testing geometry used for defining acoustic signal alarm thresholds. More information can be found in APPENDIX C.

Sensing System

The present work utilized the AE methodologies to monitor the FDM-type 3D-printing process, utilizing a piezoelectric transducer that converts mechanical energy into electrical signals. The target site for data acquisition was the 3D-printer's hot end (**Figure 5**), which includes the nozzle and has the primary function of temperature-based material deposition. The reasoning for instrumenting at the nozzle with the AE sensor was because the nozzle is always in direct contact with the part being manufactured and is useful in classifying extrusion-related defects. Additionally, any part delamination or scraping can be sensed from the nozzle as well. A user-defined acquisition threshold was defined to eliminate baseline signal noise that is not relevant for interpretation of the machine state. For the purposes of this work, a PICO sensor (MISTRAS© Group Inc, Princeton Junction, NJ) with an operating frequency range of 200-750 kHz was used. To accommodate the AE sensor, the nozzle had to be outfitted with an additional brass waveguide placed orthogonal to the material deposition direction. This enabled the sensor to be mounted in

close proximity with the heated nozzle whilst maintaining proper signal transmission. The couplant used between the waveguide and the sensor was cyanoacrylate adhesive.

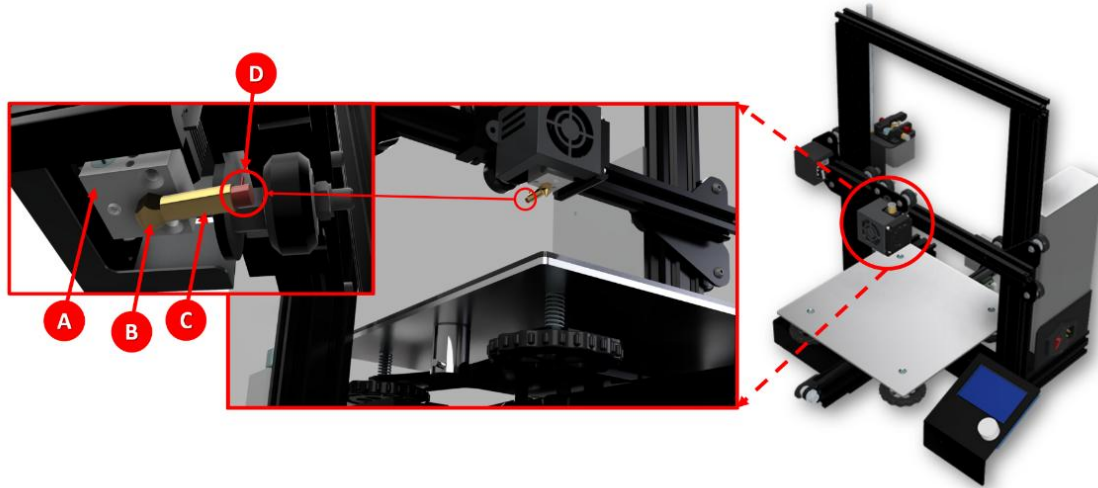


Figure 5: The FDM-type 3D-printer contains a hot end for material deposition and is comprised of A) a heat block and B) a nozzle. A C) brass waveguide was used to mount the D) AE PICO-sensor for acoustic signal acquisition.

The defects classified as under- and over-extrusion are characterized by specific visible features. A part that is under-extruded was expected to have porous regions due to insufficient material flow. The state of over-extrusion is characterized by regions that have extra material deposition. The sensor placement on the nozzle enables acquisition of signals related to the flow of melted filament, which is typically controlled by a combination of the extrusion rate and the temperature of the hot end.

The software counterpart to the PICO sensor and AE DAQ is AEwin™ (MISTRAS© Group Inc., Princeton, NJ). While this software has several functionalities, the three primary aspects were data acquisition, feature extraction, and setting up alarm triggers (APPENDIX B). The software acquires raw voltage signals from the sensor and extracts corresponding features from the data in real time. The data is also pre-processed to eliminate the impact of baseline system noise and intended motions. The features are represented in scatter plot form as raw data which is

then converted into a visualization that is defined by the user. This process of data acquisition and feature extraction within the software is detailed for the amplitude feature in **Figure 6**.

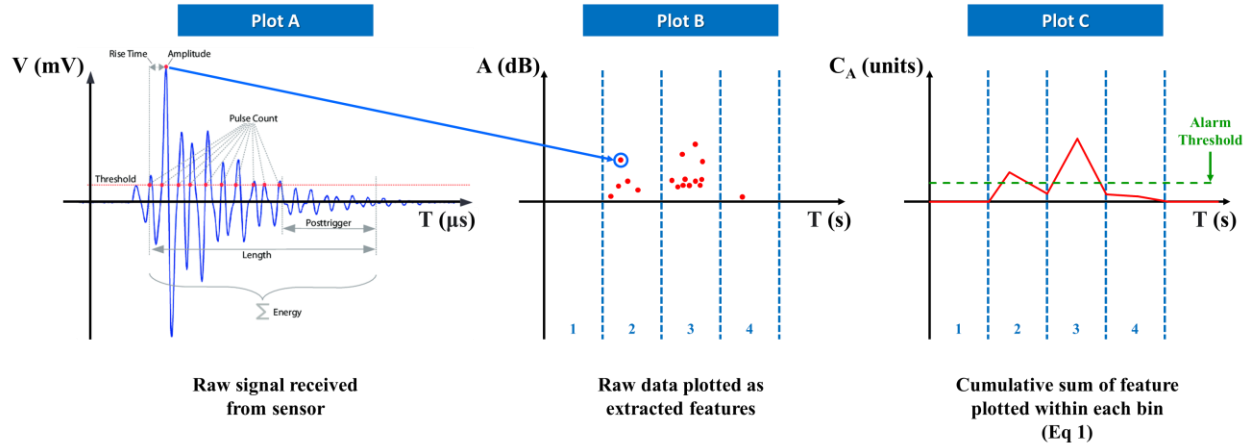


Figure 6: Graphical depiction of the AE data process for the real-time monitoring used in the closed-loop system of Figure 2

The selected data visualization method of cumulative amplitude is useful in characterizing the behavior of the system, primarily to distinguish states of normal operation (e.g., reduced number of low-amplitude data points) from states of abnormal operation (e.g., increased number of data points at amplitudes above those found in normal operation). A binned histogram was selected as the main data visualization method. The data points in Plot C of **Figure 6** were obtained using Equation 1, which plots the sum of all AE hits within a bin. The cumulative sum of amplitude (C_A) was obtained as the sum of each individual hit, i , contained within a bin, x , from Plot B of **Figure 6**.

$$C_A = \sum_i^{m_x} A_i^{(x)} \quad (1)$$

The next software aspect involved the alarm functionality based on user-defined thresholds which can be used to trigger alarms in an output log text file. The alarms were configured using the Graph Alarm functionality in the software whereby a feature such as Cumulative Amplitude can be plotted in the form of a cumulative plot. A custom threshold, as determined by experiments

explained in the Experimental Approach section, was defined to determine what level of signals must be acquired in each bin of the cumulative plot to constitute an alarm trip (APPENDIX D). Additional information related to feature plotting, alarms, and the associated triggering for the printer controller are described in the IoT Integration and Closed-Loop Control section.

IoT Integration and Closed-Loop Control

The IoT approach is comprised of the following hardware components: a data acquisition system, a data analyzer, and a printer controller labeled as a, b, c, d, and e, respectively (**Figure 2**). Monitored acoustic data is sent from the AE data acquisition (DAQ) unit (Micro-SHM, MISTRAS© Group Inc, Princeton Junction, NJ) to the AE Data Analyzer wirelessly through a local network (**Figure 2b, Figure 2c**). The AE Data Analyzer houses a Python™ environment which analyzes data file outputs from the AEwin Software. The AE Data Analyzer also houses a custom-developed watchdog script that reads the AE output data files. Output file formats include the *.DTA proprietary database file, and a converted *.TXT file (**Figure 2d**).

AEwin™ provides a configuration that allows for auto-file close after a pre-defined file size is reached. Through testing, it was determined that 35 KB sized files were adequate for near real-time detection followed by live file output. When a signal file reached 35 KB, another file was generated. The watchdog script was used to read the “chunked files” of 35 KB (**Figure 2d**) sequentially. The files themselves were structured so that they include key signal features. Moreover, the script generation was automated and therefore no human intervention was needed during a 3D-print. The watchdog script further included traffic control integration and exception handling. The script provides a line-by-line reader for the user to view signal features if AE activity was recorded.

Specifically, the watchdog script looked for alarms based on an “Amplitude Trip” defined in the AEWIn Software. This trip-type alarm for the cumulative amplitude (**Figure 6**) was outputted only if a user-defined threshold was reached. The specific threshold value was determined using training data described in subsequent sections. Based on the read alarm, the AE Data Analyzer, with the watchdog script, prompted the printer controller over the Internet (**Appendix E**). Several printing commands can be sent to the printer including pause job, change temperature, change extrude amount, set feed rate, etc. Furthermore, the watchdog script was structured for the integration of a hybridized input from multiple sensing methods, also enabling multiple control commands.

The printer controller is comprised of a cloud-based client called OctoPrint™ and its respective dependencies in Python™ and MJPG Streamer for live viewing of prints (OctoPi, 2021). OctoPrint™ receives commands from scripts on the AE Data Analyzer and the G-Code is then sent to control the printer (**Figure 2e**).

Experimental Approach

Three main experiments were conducted. The *first experiment* aimed to establish a baseline trigger for the defective prints compared to those that were pristine. A total of nine prints were produced, three each for pristine, under- and over-extrusion cases. For this experiment, the defect region of the over- and under-extruded parts were specifically localized between layers 27 to 53 (**Figure 7A**). The defective segment was chosen to be in the middle third of the trapezoidal test geometry, which consisted of 81 total print layers. This defective range was used to match the timing of the acoustic signal range to ensure comparability between pristine and defective prints. During the print, time markers for critical events were recorded in AEWIn™ at layers 1 (first layer), 3, 27, 53 and 81(last layer). Alarm triggers were produced and annotated in the 35KB files produced by the AE Data Analyzer. The watchdog script then read through the data files and in

the presence of an alarm line, executed a sequence of user-defined corrective actions through the printer controller.

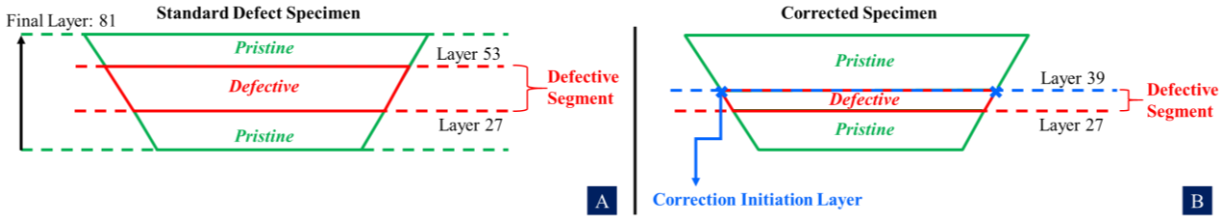


Figure 7: Schematic of the localization of the induced defect region in terms of layer height, as per the first experiment (A). Schematic of region with reduced defect region size due to the execution of corrective actions, as per the second experiment (B).

For the *second experiment*, once the baseline signals for the pristine and defective trapezoidal test geometries was established, the closed-loop control system was tested using manually instigated acoustic signal spikes, resulting in the deliberate triggering of alarms in the AE Analyzer. Once a defective print started and the watchdog script began monitoring files, correction scripts were executed due to manual alarm triggering when the X-axis gantry was physically tapped (**Figure 5**). The physical tapping was introduced when the print reached layer 39 (**Figure 7B**), which is directly before the midway point of the defective segment, ensuring that the alarm signal was properly recorded. The watchdog script corrected the defect by introducing a control script to revert the flow rate back to 100%, thereby returning to the pristine state for the remaining layers. Once this was completed, the *third experiment* involved running a defective print at the established threshold and letting the correction script run autonomously with no manual instigation.

Results

Experiment 1: Alarm-defining prints and threshold values determination

Three experimental datasets each of pristine, over-extruded, and under-extruded print data, were collected to define the alarm thresholds. The signal regions between layers 27-53 represented the defective segments (**Figure 7A**). In this context, **Figure 8** shows representative data acquired for the nine total prints of the trapezoidal test geometry. The data was plotted as 2D cumulative histogram of the cumulative sum of amplitude. These plots have 50 bins that were populated throughout the course of the print. These were populated with cumulative amplitude as per the data visualization method described in **Figure 6**. The focus in the presented analysis was to define differences between the cumulative amplitude across the pristine and defective prints in the portion of the graph labeled “3”. Some outliers, marked with an “X”, occurred towards the end of the 3D-prints and were associated to printing issues unrelated to the experiments.

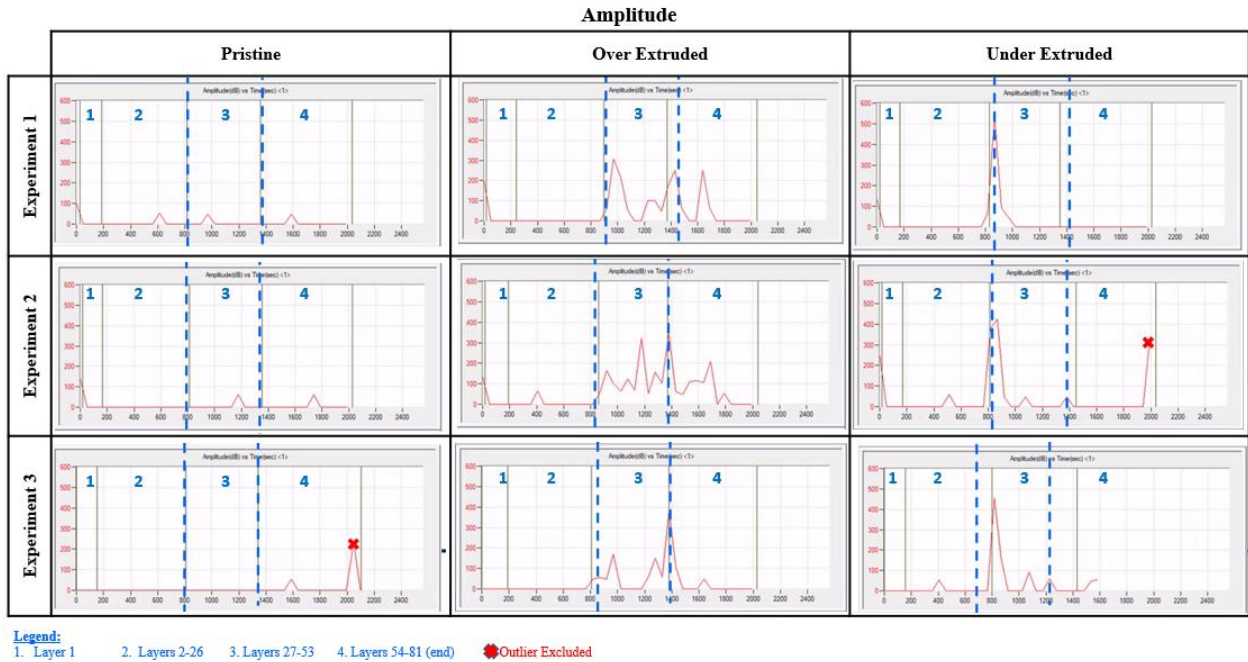


Figure 8: Representative AE monitoring signals plotted as cumulative amplitude sum (amplitude units) versus time (seconds) for pristine, over- and under-extruded prints of the trapezoidal test geometry.

Table 1 shows the average cumulative amplitude threshold values, determined based on these prints. Since the graphs were time-stamped, the table also includes an average peak cumulative amplitude value for each of the layers defined in **Figure 7**. The defective range for comparison is layers 27-53.

Table 1: Alarm threshold values defined based on data similar to the ones shown in **Figure 8**

Alarm Threshold Values				
Classification	Layer(s)	Pristine	Over Extruded	Under Extruded
Pristine	1	0	0	0
Pristine	2-26	16.67	16.67	33.33
Defective	27-53	36.67	340	463.33
Pristine	54-81	53.33	166.67	16.67
Recommended Threshold Alarm			150	

Experiment 2: Control System Demo

A sample dataset involving triggering the alarm by tapping on the X-axis gantry of the 3D-printer is shown in **Figure 9**. The transition point at layer 39 (introduction of manual tapping) was marked with a blue dot (**Figure 9**). After the alarm signal is generated in the AEwin™ software, a text file containing an alarm line is outputted and subsequently read by the watchdog script. An operational command, predefined using a control script, was then sent to the 3D-printer via the OctoPrint™ interface.

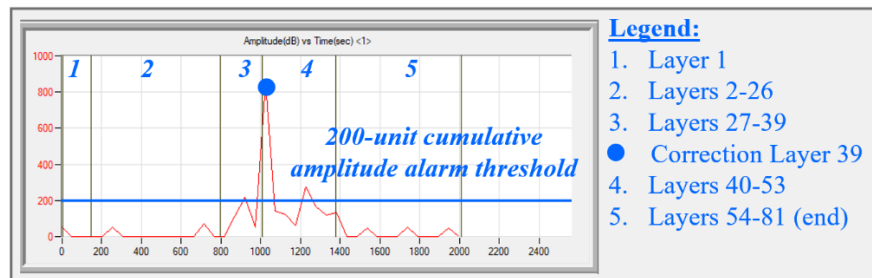


Figure 9: AE data for over-extruded test print that was intercepted and corrected by physically tapping the X-axis gantry midway through the defect segment (layer 39)

Experiment 3: Autonomous 3D-printing closed-loop monitoring system demonstration

The third experiment involved standalone testing of the entire control loop. Using the obtained thresholds and the correction script from the experiments described above, an autonomous print was conducted which involved no manual instigation at the alarm trigger site. A spike in the defect segment of the AE data in **Figure 9** was successfully identified based on the newly defined threshold values and was able to trigger an alarm which independently initiated the correction process. As described in the Experimental Approach section, the correction script reverted the flow rate of the print to 100%, causing the remaining portion of the sample to match that of a pristine part. The results of this autonomous demonstration are shown in **Figure 10** in which the corrected sample for each respective over- and under-extrusion defect is compared to the corresponding non-corrected prints. This work demonstrated the interconnection of manufacturing, data acquisition/analysis, and control under one closed-loop monitoring system. This system utilized a desktop-class FDM 3D-printer to prove the feasibility and usefulness of the workflow in the larger context of in-situ monitoring of manufacturing processes.

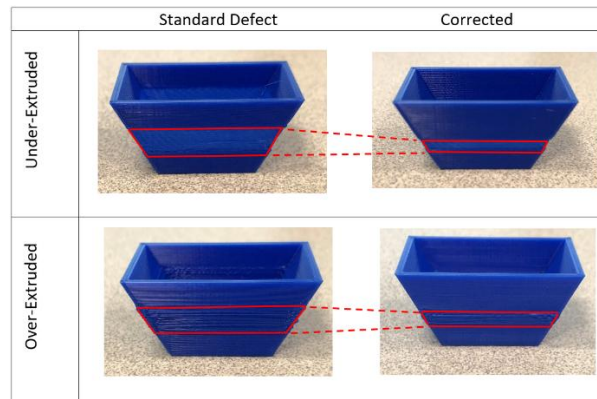


Figure 10: Physical model comparison of standard and corrected sample prints for over and under-extruded prints

Discussion

The closed-loop feedback control system explored in this work is representative of an IoT framework and live workflow to acquire data from a variety of sources and processes, while also providing a way to interpret the data in the context of operation and take corrective actions. For this work, a 3D-printer was used as a proof of concept to demonstrate this approach. This framework can be adopted for alternative hardware solutions and the workflow itself can be adapted to subtractive manufacturing machines such as CNC mills, among others.

The experiments conducted to establish the threshold for the alarm and the subsequent demonstration of the entire control loop further establish the need for an efficient and optimized in-situ monitoring system. As shown in the plots of the acquired data, even in a controlled environment, there is variability across multiple prints of the same geometry. With a larger sample size, this variability is expected to become more defined.

There are several benefits to using AE as a monitoring method for 3D-printers, including real-time data acquisition and processing. Additionally, AE monitoring has minimal impact to the ongoing operations of the printer, allowing for instrumentation at several critical locations. Some drawbacks to relying solely on AE sensors relate to the ability to classify the global health of the printer. In many cases AE provides a qualitative assessment of a portion of the ongoing process. As a result, augmenting the developed monitoring system by incorporating additional data sources such as optical, thermal, or vibrational could significantly enhance the extracted information about the health of the process and the overall system's capabilities. This information can be further used to take additional actions to address defective states. As an example, *Figure 11* showcases an expanded workflow that incorporates an additional optical data source. In the specific context of 3D-printing, if a defect is detected, the parameters (e.g., temperature, flow rate, position) of the

printer can be tuned live, enabling an operator to potentially correct or abort the print without sacrificing excess material.

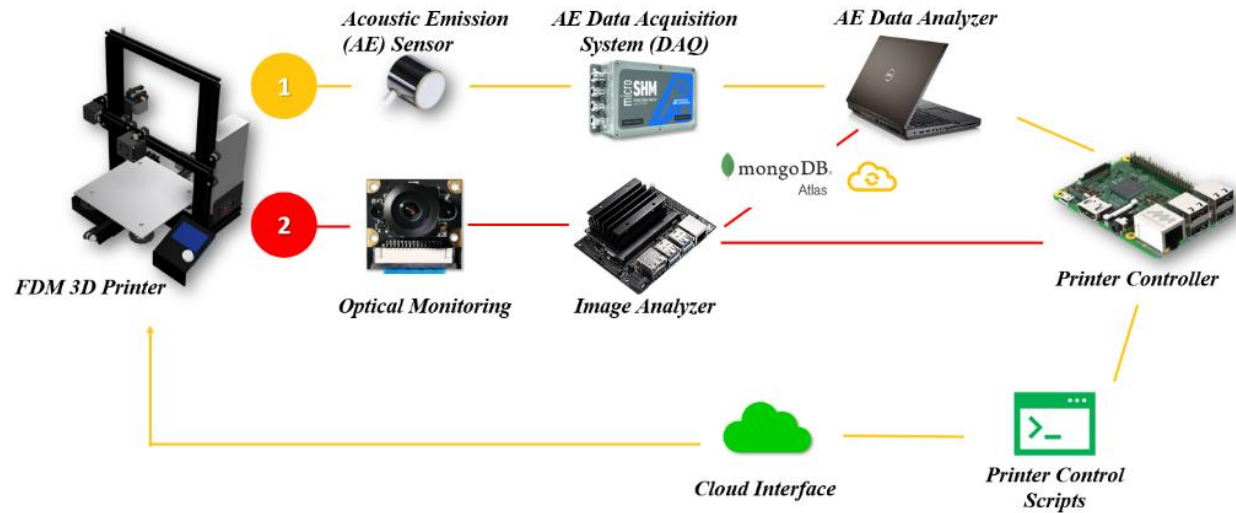


Figure 11: Expanded workflow with additional optical sensing source for hybridized monitoring approach

Conclusion

Moving forward, this work will expand its scope to include additional data sources for monitoring a manufacturing process, including optical, thermal, and vibrational sensors. To effectively develop a hybridized sensing approach using these extrinsic devices, a comprehensive IoT framework will be needed. Additionally, the integration of a database for sensor data, such as MongoDB™ (cross-platform document-oriented database program), will be important for future developments as this provides simple retrieval and aggregation of data. A flexible schema will need to be developed to integrate data from multiple sensing inputs. The analysis will also take advantage of machine learning methods to further diagnose printing faults based on training data. The present team aims to support the collective goal in industry of creating a modeling-level approach that can effectively diagnose a machine's process and effectively triage appropriate reactive action commands/sequences.

ACKNOWLEDGEMENTS

The efforts of members of the Theoretical and Applied Mechanics Group to support this work are greatly appreciated.

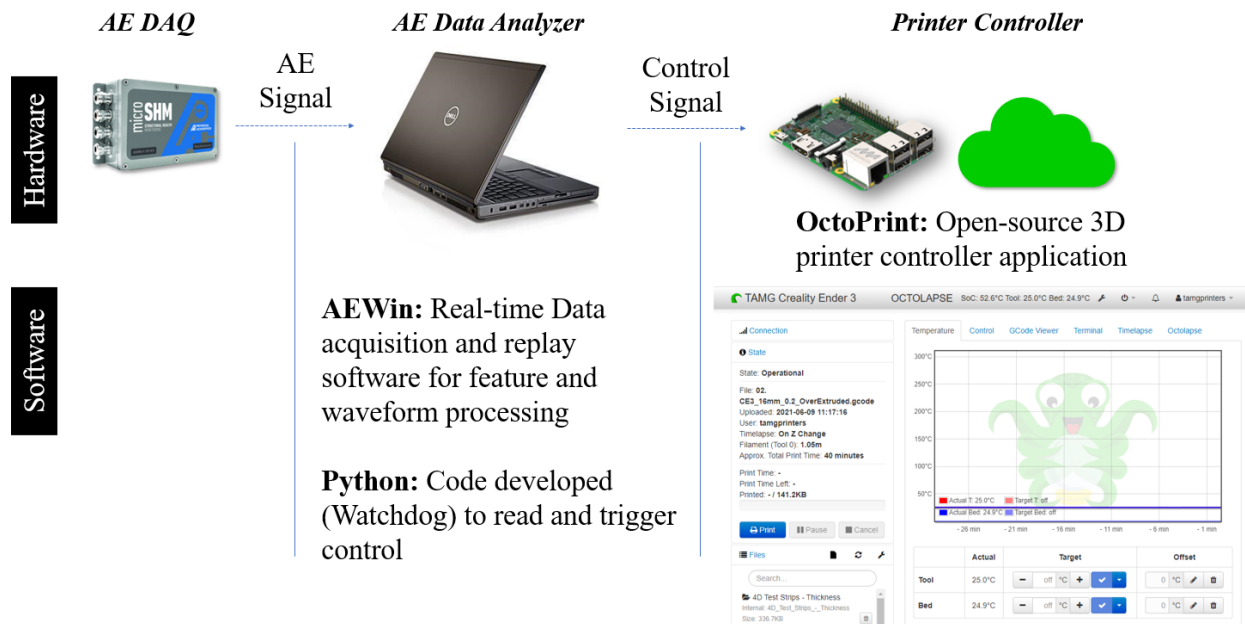
APPENDIX A

Table A-1: System Components – Bill of Materials

Component	Manufacturer	Link
Hardware		
Ender 3 Pro	Creality	Creality
Micro-SHM	MISTRAS	Physical Acoustics
AE PICO Sensor	MISTRAS	Physical Acoustics
Loctite Adhesive	LOCTITE	Digikey
Raspberry Pi Model 3 B+	Raspberry Pi	Raspberry Pi
Raspberry Pi Camera	Raspberry Pi	Raspberry Pi
PLA 1.75mm Filament	Hatchbox	Hatchbox
Dell Precision 4800	Dell	Dell
Software		
Python Environment	Python	Python
OctoPrint Client	OctoPrint	OctoPrint

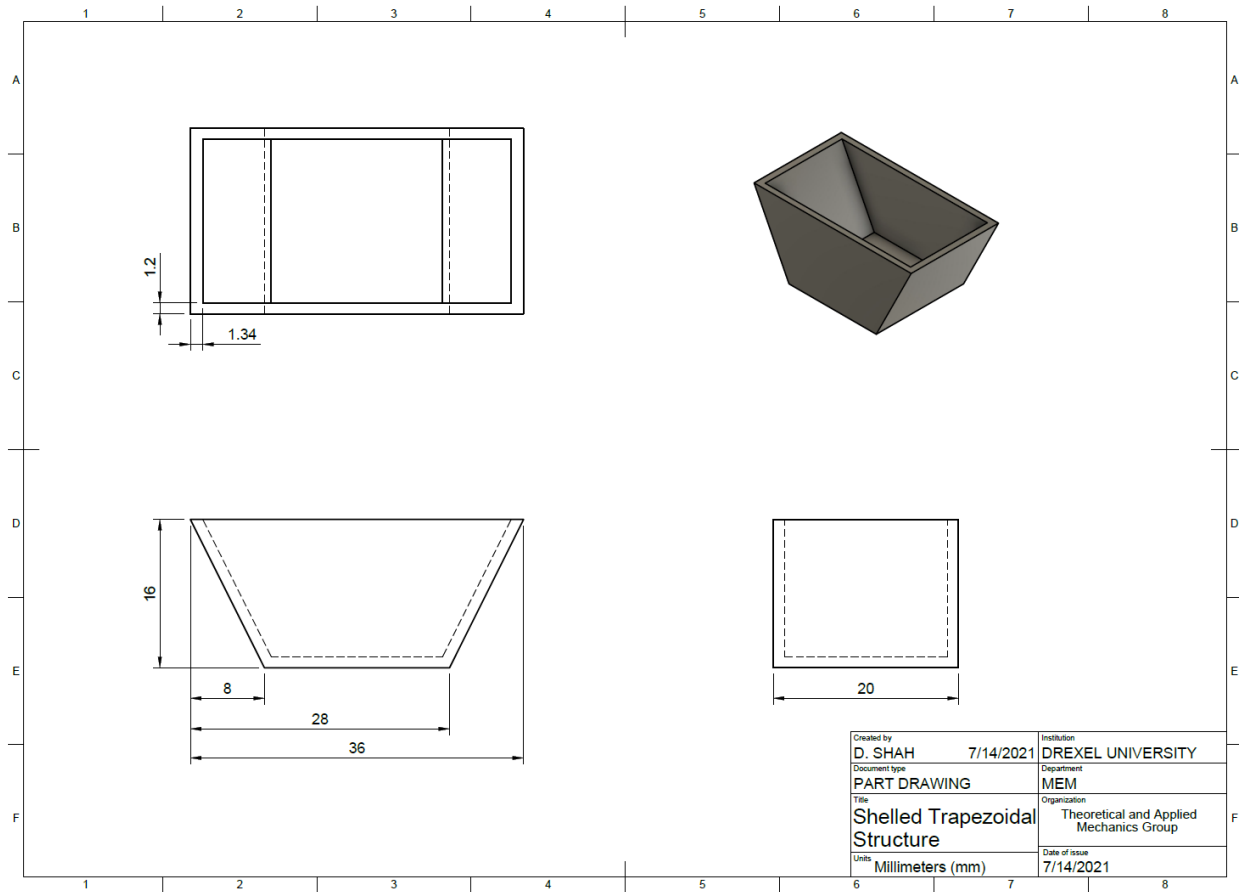
APPENDIX B

Figure B-1: Diagram for IoT Software and Hardware Components



APPENDIX C

Figure C-1: Engineering Drawing for trapezoidal testing geometry



APPENDIX D

Figure D-1: AEwin Acquisition Parameters

Parameter	Value	Notes
Acquisition Threshold	45 dB	Defined to limit noise input from printer motion
PDT/HDT/HLT	400/800/800 μ s	Obtained based on PLB test after sensor is mounted
File Auto-Close	35 KB	Defined to get nearly instantaneous alarm responses
Alarm Threshold	150 units	Threshold defined to differentiate between pristine/defective

Figure D-2: AEwin Parameters for Acquisition Threshold

AE Channel Setup			
Preamp			
Sensors, Filters and Waveforms			
AE Channel	Threshold		
	Type	dB	FTBnd
<input checked="" type="checkbox"/> 1	FIXED	45	6

Figure D-3: Parameters for Graph Alarms

Graph Setup

Channels | Event Groups | Clustering | Misc. | **Alarms**

☒ Enable Graph Alarm ☐ Enable Warning Level: 0

Y Axis to Monitor: Primary ☒ Enable Trip Level: 60

☐ Alarm Hold Off # Signals: 1

OK Cancel Apply

Type: 2D Histogram

Y (Vertical) Axis: Primary

Amplitude

☐ One per Channel

0 Minimum 10 Maximum

☐ Log Scale ☐ Invert

☐ Manual (Fixed) ☒ Compress ☐ Slide

Input Data: ☐ No Hits or Events ☒ Hits ☐ Events ☐ Ast Hits ☐ Include Time Driven

☒ Show Grid

Preview

X (Horizontal) Axis: Primary

Time

0 Minimum 10 Maximum

☐ Log Scale ☐ Invert

☐ Manual (Fixed) ☒ Compress ☐ Slide ☐ Expand

Value Axis: ☒ Y-Axis ☐ X-Axis

None Cumulate

Bin Axis: 50 # of Bins

Bin Display: ☒ Sum ☐ Minimum ☐ Average ☐ Maximum ☐ Rate ☐ Min-Max ☐ Real Time

Simple Line

☐ Polynomial Curve Fit

1:1 Aspect Ratio ☐

Figure D-4: AEwin Timing Parameters

AE Channel Setup				
Preamp				
Sensors, Filters and Waveforms				
AE Timing Parameters				
Data Sets/Parameters				
AE Channel	PDT	HDT	HLT	Max Duration
	microseconds	microseconds	microseconds	milliseconds
<input checked="" type="checkbox"/> 1	400	800	800	99

Figure D-5: AEwin Acquisition Sampling Parameters

AE Channel Setup Preamp Sensors, Filters and Waveforms AE Timing Parameters Data Sets/Parameters Parametric Setup Front End Filters Front End Alarms								
AE Channel	Sensor	Analog Filter		Digital Filter		Waveform Setup		
		Lower	Upper	Lower	Upper	Sample Rate	Pre-Trigger	Length
<input checked="" type="checkbox"/> 1	15	20kHz	1MHz	None	None	1MSPS	256.0000	1k

Figure D-6: AEwin Configuration of Auto File-Close

Set Auto File-Close Criteria

☐ Close/Reopen on Hits

☐ Enable # Hits:

☐ Close/Reopen on Elapsed Time

☐ Enable Elapsed Time Days: Hours: Min: Sec:

☒ Elapsed timer begins at test start.

☐ Elapsed timer begins at specified time of day (set below)

Time of day: Hour: Min: (24 hr clock)

☐ Close/Reopen on File Size

☐ Enable File Size: kilobytes

☒ Use Continued Files

☐ Save Layout On Auto-Close

OK Cancel

Figure D-7: AEwin Features Selected for Export

AE Channel Setup | Preamp | Sensors, Filters and Waveforms | AE Timing Parameters | Data Sets/Parameters | Parametric Setup | Front End Filters | Front End Alarms

Hit Data Set:

☒ Amplitude ☐ Average Frequency

☒ Energy ☐ Reverberation Frequency

☒ Counts ☐ Initiation Frequency

☒ Duration ☐ Signal Strength

☐ RMS ☒ Absolute Energy

☐ ASL

☐ Threshold

☒ Rise Time

☐ Counts to Peak

Hit Parameters:

☐ 1 ☐ 2

Spectrum Features:

☒ Frequency Centroid

☒ Peak Frequency

☐ Partial Power

0 Segments Defined

Time Driven Parameters:

☐ 1 ☐ 2

Time Driven Channel Data:

☐ RMS ☒ ASL

☐ Threshold ☐ Absolute Energy

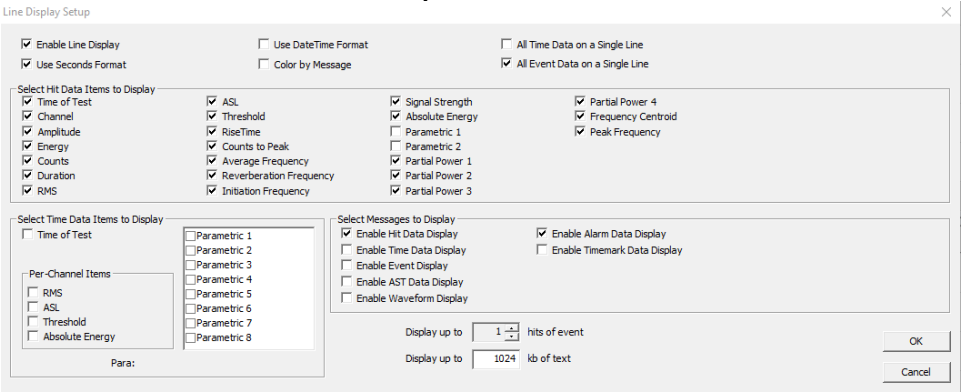
Time Driven Rate: sec ☒ seconds ☐ milliseconds

Constants:

RMS/ASL Time Constant: ms

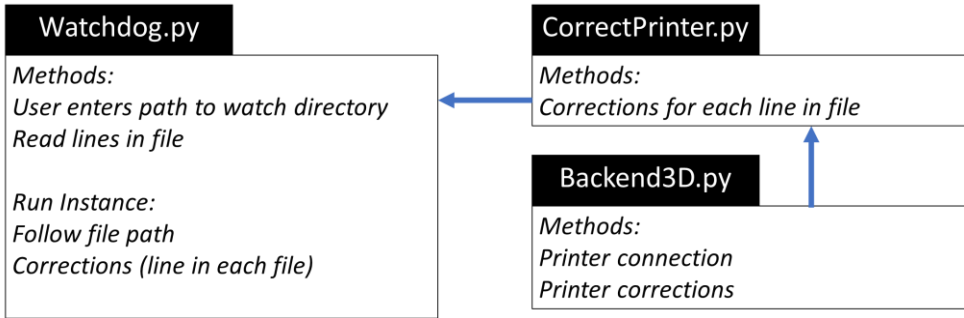
Energy Reference Gain: dB

Figure D-8: AEwin Features Defined for Export



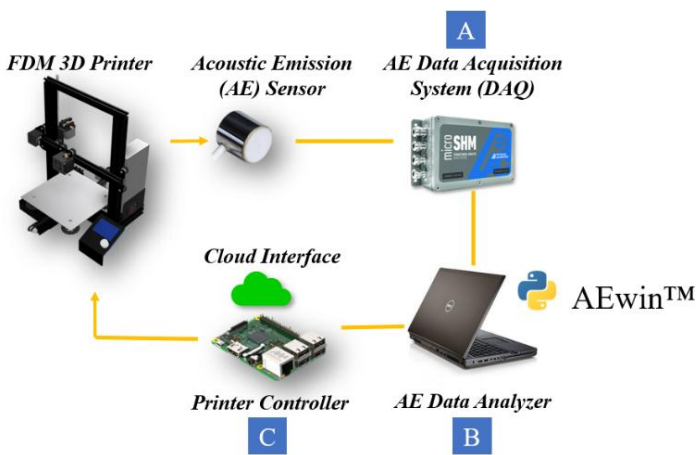
APPENDIX E

Figure E-1: Representative diagram of watchdog script



APPENDIX F

Figure F-1: Hardware Specs



Reference Component	Hardware
A	The Micro-SHM is a standalone acoustic emission (AE) system made by Physical Acoustics.
B	Dell Precision M4800 laptop with an i7 Intel Core processor and 64-bit operating system for Windows. AEwin is a Windows-based program for real-time feature and waveform processing, display and control with MISTRAS AE systems [24]
C	A Raspberry Pi B+ with a 64-bit quad core processor with OctoPi (Raspbian based SD Card image).

References

- Bacha, A., Sabry, A. H., & Benhra, J. (2019). Fault Diagnosis in the Field of Additive Manufacturing (3D Printing) Using Bayesian Networks. *International Journal of Online & Biomedical Engineering*, 15(3).
- Chen, T., & Wang, Y.-C. (2019). An advanced IoT system for assisting ubiquitous manufacturing with 3D printing. *The International Journal of Advanced Manufacturing Technology*, 103(5), 1721-1733.
- Commission, E. (2021). Advanced Technologies for Industry. *Internal Market, Industry, Entrepreneurship and SMEs*. Retrieved from <https://ati.ec.europa.eu/>
- Delli, U., & Chang, S. (2018). Automated process monitoring in 3D printing using supervised machine learning. *Procedia Manufacturing*, 26, 865-870.
- Do, N. (2017). Integration of design and manufacturing data to support personal manufacturing based on 3D printing services. *The International Journal of Advanced Manufacturing Technology*, 90(9), 3761-3773.
- Ferraris, E., Zhang, J., & Van Hooreweder, B. (2019). Thermography based in-process monitoring of Fused Filament Fabrication of polymeric parts. *CIRP Annals*, 68(1), 213-216. doi:<https://doi.org/10.1016/j.cirp.2019.04.123>
- Fu, Y., Downey, A., Yuan, L., Pratt, A., & Balogun, Y. (2020). In situ monitoring for fused filament fabrication process: A review. *Additive Manufacturing*, 38, 101749. doi:10.1016/j.addma.2020.101749
- Gaja, H., & Liou, F. (2017). Defects monitoring of laser metal deposition using acoustic emission sensor. *The International Journal of Advanced Manufacturing Technology*, 90(1-4), 561-574.
- Garanger, K., Khamvilai, T., & Feron, E. (2018). *3D printing of a leaf spring: A demonstration of closed-loop control in additive manufacturing*. Paper presented at the 2018 IEEE conference on control technology and applications (CCTA).
- Kennedy, S. (2015). Made in China 2025. *Critical Questions*. Retrieved from <https://www.csis.org/analysis/made-china-2025>
- Liu, J., Hu, Y., Wu, B., & Wang, Y. (2018). An improved fault diagnosis approach for FDM process with acoustic emission. *Journal of manufacturing processes*, 35, 570-579. doi:10.1016/j.jmapro.2018.08.038
- Lu, Q. Y., & Wong, C. H. (2018). Additive manufacturing process monitoring and control by non-destructive testing techniques: challenges and in-process monitoring. *Virtual and Physical Prototyping*, 13(2), 39-48. doi:10.1080/17452759.2017.1351201
- Meng, L., McWilliams, B., Jarosinski, W., Park, H.-Y., Jung, Y.-G., Lee, J., & Zhang, J. (2020). Machine learning in additive manufacturing: A review. *Jom*, 72(6), 2363-2377.
- Menon, A., Póczos, B., Feinberg, A. W., & Washburn, N. R. (2019). Optimization of silicone 3D printing with hierarchical machine learning. *3D Printing and Additive Manufacturing*, 6(4), 181-189.
- OctoPi. (2021). Download & Setup OctoPrint. Retrieved from <https://octoprint.org/download/>
- Rao, P. K., Liu, J., Roberson, D., Kong, Z., & Williams, C. (2015). Online Real-Time Quality Monitoring in Additive Manufacturing Processes Using Heterogeneous Sensors. *Journal of manufacturing science and engineering*, 137(6). doi:10.1115/1.4029823
- Reese, R., Bheda, H., & Mondesir, W. (2019). Method to monitor additive manufacturing process for detection and in-situ correction of defects. In: Google Patents.

- Tlegenov, Y., Lu, W. F., & Hong, G. S. (2019). A dynamic model for current-based nozzle condition monitoring in fused deposition modelling. *Progress in Additive Manufacturing*, 4(3), 211-223. doi:10.1007/s40964-019-00089-3
- Wang, C., Tan, X., Tor, S., & Lim, C. (2020). Machine learning in additive manufacturing: State-of-the-art and perspectives. *Additive Manufacturing*, 101538.
- Wang, T., Kwok, T.-H., Zhou, C., & Vader, S. (2018). In-situ droplet inspection and closed-loop control system using machine learning for liquid metal jet printing. *Journal of manufacturing systems*, 47, 83-92.
- Wang, Y., Lin, Y., Zhong, R. Y., & Xu, X. (2019). IoT-enabled cloud-based additive manufacturing platform to support rapid product development. *International Journal of Production Research*, 57(12), 3975-3991.
- Wu, H., Wang, Y., & Yu, Z. (2016). In situ monitoring of FDM machine condition via acoustic emission. *The International Journal of Advanced Manufacturing Technology*, 84(5-8), 1483-1495.
- Wu, H., Yu, Z., & Wang, Y. (2016). *A new approach for online monitoring of additive manufacturing based on acoustic emission*. Paper presented at the International Manufacturing Science and Engineering Conference.
- Wu, H., Yu, Z., & Wang, Y. (2019). Experimental study of the process failure diagnosis in additive manufacturing based on acoustic emission. *Measurement : journal of the International Measurement Confederation*, 136, 445-453. doi:10.1016/j.measurement.2018.12.067
- Wu, M., Phoha, V. V., Moon, Y. B., & Belman, A. K. (2016). *Detecting malicious defects in 3d printing process using machine learning and image classification*. Paper presented at the ASME International Mechanical Engineering Congress and Exposition.
- Yoon, J., He, D., & Van Hecke, B. (2014). *A PHM approach to additive manufacturing equipment health monitoring, fault diagnosis, and quality control*. Paper presented at the Proceedings of the prognostics and health management society conference.